

Almiramides A–C: Discovery and Development of a New Class of Leishmaniasis Lead CompoundsLaura M. Sanchez,[†] Dioxelis Lopez,[‡] Brian A. Vesely,^{||} Gina Della Togna,[‡] William H. Gerwick,[§] Dennis E. Kyle,^{||} and Roger G. Linington^{*†}

[†]Department of Chemistry and Biochemistry, University of California Santa Cruz, 1156 High Street, Santa Cruz, California 95064, [‡]Instituto de Investigaciones Científicas Avanzadas y Servicios de Alta Tecnología, INDICASAT, Clayton, Edificio 175, P.O. Box 7250, Panamá 5, Panamá, [§]Center for Marine Biotechnology and Biomedicine, Scripps Institution of Oceanography and Skaggs School of Pharmacy and Pharmaceutical Sciences, University of California San Diego, La Jolla, California 92093, and ^{||}Department of Global Health, College of Public Health, University of South Florida, 3720 Spectrum Boulevard, Suite 304, Tampa, Florida 33612

Received February 26, 2010

Leishmaniasis is a debilitating disease caused by protozoan parasites of the genus *Leishmania*, which affects an estimated 12 million people worldwide. The discovery of new lead compounds for leishmaniasis is therefore a pressing concern for global health programs. The organic extract of a Panamanian collection of the marine cyanobacterium *Lyngbya majuscula* showed strong in vitro activity in two complementary screens against the tropical parasite *Leishmania donovani*, the causative agent of visceral leishmaniasis. Chromatographic separation of this complex mixture led to the isolation of the highly N-methylated linear lipopeptides, almiramides A–C (**1–3**). Comparison with the biological activities of a number of related metabolites and semisynthetic derivatives revealed key features required for activity and afforded one new compound (**11**) with superior in vitro activity. Subsequent synthesis of a library of simplified analogues led to the discovery of several compounds with improved therapeutic indices to the natural products.

Introduction

Leishmaniasis is a debilitating disease prevalent across many of the intertropical regions of the world including India, Sudan, and Brazil.^{1–3} Caused by over 20 species of related intracellular parasites from the genus *Leishmania*, leishmaniasis can present itself in a number of different clinical manifestations including cutaneous, mucosal, and visceral forms of the disease.⁴ Both the cutaneous and mucosal forms can cause severe disfigurement to patients, including ulcerative skin lesions and the destruction of the mucous membranes of the nose, mouth, and throat, leading to permanent disfigurement and frequently social ostracization.⁵ However, it is the visceral form of the disease that represents the greatest threat to human health, with symptoms ranging from fever and weight loss in the initial stages to the development of hepatosplenomegaly (a dramatic enlargement of the liver and spleen) and ultimately multisystem infection and death in untreated cases. Visceral leishmaniasis is caused by a small subgroup of the *Leishmania* parasites, principally *L. donovani*, *L. infantum*, and *L. chagasi*. Current treatment is limited to only a few viable alternatives, each of which suffers from drawbacks in terms of efficacy, toxicity, or cost. Until recently, the most widely used therapeutic in most regions of the world was the pentavalent antimony-based drug sodium stibogluconate.³ Though initially highly efficacious, with an estimated 90–95% cure rate in most areas after its introduction in the 1950s, this treatment has suffered from the increasing emergence of resistance, fueled by the high rate of patient noncompliance due to the exceedingly long treatment

period and to the relatively high toxicity of this treatment regimen. More recently, alternative therapeutics have become prevalent as first line treatments. These include liposomal amphotericin B, which is highly effective and requires only a short course of treatment but is too expensive to be a viable treatment option in most developing nations, and miltefosine, an alkylphospholipid recently licensed for use against visceral leishmaniasis in India, Germany, and Colombia that has shown excellent cure rates but that is already facing instances of resistance in some areas. This shortfall of affordable and efficacious treatments has led the World Health Organization to designate leishmaniasis as a category 1 disease, signifying that it is an emerging and uncontrolled global health problem. There is therefore a pressing need for the development of new drugs to treat leishmaniasis, and it is with this aim that the Panama International Cooperative Biodiversity Group (ICBG⁶) is investigating Panamanian microorganisms for lead compounds with antileishmanial activity.^{6,7}

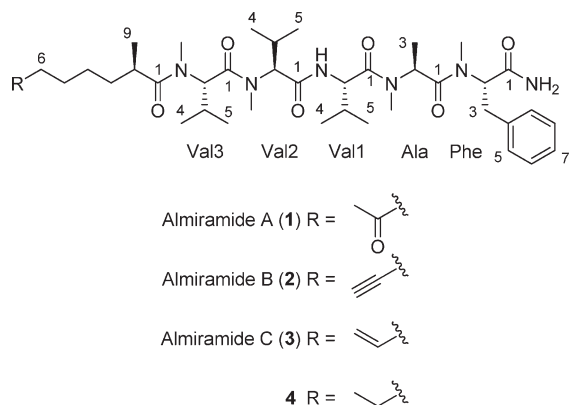
Discussion

Screening of over 400 prefractions from 40 field collections of marine cyanobacteria revealed one fraction from a collection of *Lyngbya majuscula* from the Bocas del Toro Marine

*To whom correspondence should be addressed. Phone: (831) 459-3014. Fax: (831) 459-2935. E-mail: rogerl@chemistry.ucsc.edu.

⁶Abbreviations: ICBG, International Cooperative Biodiversity Groups; RP-HPLC, reversed phase high performance liquid chromatography; HRESITOFMS, high resolution electrospray ionization time-of-flight mass spectrometry; DLVA, *N*_α-(2,4-dinitro-5-fluorophenyl)-L-valinamide; ER, enoyl reductase; SAM, S-adenosyl methionine; PKS-NRPS, polyketide synthase–nonribosomal peptide synthetase; SPPS, solid phase peptide synthesis; DIPEA, diisopropylethylamine; TIPS, triisopropylsilyl; HBTU, *O*-benzotriazol-1-yl-*N,N,N'*-tetramethyluronium hexafluorophosphate; TFA, trifluoroacetic acid; SAR, structure–activity relationship.

Park on the Caribbean coast of Panama that exhibited a unique profile against *L. donovani* without showing significant cytotoxicity to mammalian Vero cells. This combination of results indicated the presence of compounds with an intriguing biological profile and prompted us to undertake a further investigation of the mixture. Purification by C₁₈ reversed-phase (RP) solid phase extraction chromatography (50% MeOH/H₂O to 100% MeOH) afforded two consecutive active fractions that were further purified by C₁₈ RP-HPLC to give almiramides A–C (**1–3**) as optically active white solids.



Initial NMR analysis of almiramide A (**1**) in CD₂Cl₂ gave spectra that contained resonances for **1** in two distinct conformations (3:2 ratio). Reacquisition of these spectra in CD₃CN afforded spectra that also contained two conformations, though in a more acceptable ratio of 6:1. Despite the complexity of interpreting spectra for compounds that exhibit multiple stable conformers on the NMR time scale, it was possible to identify the presence of subunits **a–f** (Figure 1) using standard two-dimensional NMR techniques (Supporting Information).

HRESITOFMS gave an [M + H]⁺ pseudomolecular ion at 743.5062 that was consistent with the molecular formula C₄₀H₆₆N₆O₇ (calcd 743.5065), indicating that subunits **a–f** contained the required number of double bond equivalents and that **1** was a linear lipopeptide. Careful consideration of both HMBC and ROESY data for these subunits as indicated in Figure 1 allowed for the construction of the planar structure of **1**. This assignment was further supported by the fragmentation pattern in the atmospheric pressure chemical ionization (APCI) mass spectrum, which was consistent with the connectivity determined via the NMR data (data not shown). In particular, the fragmentation data showed a loss of 17 amu that is a characteristic diagnostic for terminal amide functional groups due to a neutral loss of NH₃ and gave additional confirmation for the assignment of subunit **f**.

Almiramide B (**2**) gave a HRESITOFMS [M + H]⁺ pseudomolecular ion at 725.4964 that was consistent with the molecular formula C₄₀H₆₄N₆O₆ (calcd 725.4960). cursory examination of the proton spectrum for **2** showed it to possess the same gross structure as **1**. A more detailed consideration of the NMR data showed **2** to possess the same peptidic portion as found in **1**, implying that the structural variation lay in the lipid side chain. The absence of the methyl singlet and ketone carbonyl signals from **1** (δ_H 2.04, δ_C 29.9, and δ_C 209.6, respectively), combined with the presence of new quaternary carbon (δ_C 85.4) and methyne signals (δ_H 2.16, δ_C 69.7) for **2**,

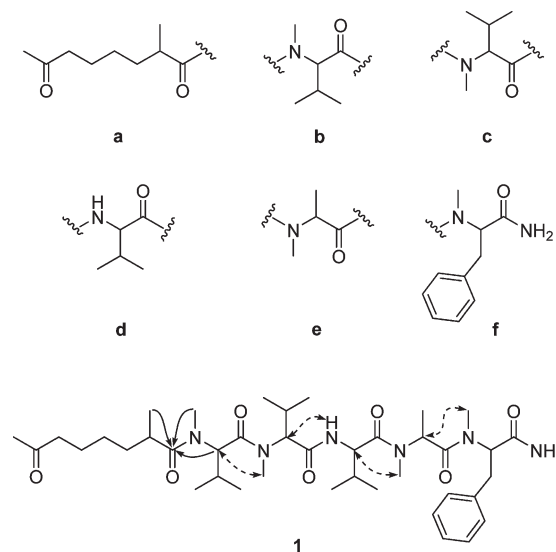


Figure 1. Subunits **a–f** and NMR connectivity for **1**. Solid arrows indicate HMBC correlations. Dashed arrows indicate ROESY correlations.

strongly suggested that the terminal ketone of **1** had been replaced with a terminal alkyne in **2**. Further consideration of the NMR data for this compound (Table 1) confirmed this initial assignment, through a combination of COSY and HMBC correlations.

Almiramide C (**3**) gave a HRESITOFMS [M + H]⁺ pseudomolecular ion at 727.5115 that was consistent with the molecular formula C₄₀H₆₆N₆O₆ (calcd 727.5116). As with almiramide B, consideration of the NMR resonances for the amino acid residues present in **3** showed them to be identical to those for almiramide A (**1**), suggesting that **3** differed from **1** and **2** in the constitution of the lipophilic side chain. The presence of three new multiplet proton resonances between δ_H 4.89 and δ_H 5.83 and new resonances in the carbon spectrum at δ_C 115.0 and δ_C 140.1, coupled with the absence of the quaternary carbon (δ_C 85.4) and methyne signals (δ_H 2.16, δ_C 69.7) for **2**, suggested the presence of a monosubstituted olefin in place of the terminal alkyne present in **2**. This assignment was confirmed by consideration of the gCOSY, gHSQC, and gHMBC spectra for **3** that unequivocally identified the fatty acid terminus as a 2-methyloct-7-enoic acid residue.

Determination of the complete absolute configuration for **1–3** was accomplished using two complementary approaches (Scheme 1). For the amino acid residues, advanced Marfey's analysis was employed⁸ and the resulting derivatives analyzed by LC–MS. For the determination of the configuration at the 2-position of the side chain, compounds **2** and **3** were hydrogenated to form compound **4** and hydrolyzed to afford the free fatty acid, which was subsequently derivatized with a chiral derivatizing agent and compared to synthetic standards by GC–MS.

It has been noted that side chains containing a terminal alkyne moiety are not stable to the strongly acidic conditions typically employed in the hydrolysis of peptides.⁹ Consequently, both **2** and **3** were subjected to hydrogenation over palladium on carbon to form compound **4** prior to hydrolysis. The hydrolysis products were partitioned between 0.1 N HCl and EtOAc to afford the amino acids in the aqueous phase and the lipid chain in the organic phase. The aqueous portions from all three samples were separately concentrated to dryness in vacuo. The resulting amino acid residues were derivatized

Table 1. NMR Data for Almiramides A–C (1–3) (CD₃CN)

residue	position	1			2			3		
		δ_{H}^a	mult, <i>J</i> (Hz)	δ_{C}^b	δ_{H}^a	mult, <i>J</i> (Hz)	δ_{C}^b	δ_{H}^a	mult, <i>J</i> (Hz)	δ_{C}^b
Phe	NH ₂	5.81, 6.26	bs, bs		5.80, 6.26	bs, bs		5.79, 6.26	bs, bs	
	1			172.9			173.0			173.0
	2	5.44	dd, 4.4, 12.1	58.5	5.44	dd, 4.4, 12.1	58.6	5.44	dd, 4.4, 12.1	58.6
	3	2.95, 3.33	m dd, 4.8, 15.0	34.5	2.95, 3.31	m dd, 4.8, 15.0	34.6	2.94, 3.31	m dd, 4.8, 15.0	34.7
	4			138.9			139.1			139.1
	5	7.23	m	129.9	7.23	m	130.0	7.23	m	130.0
	6	7.28	m	129.5	7.27	m	129.5	7.27	m	129.6
	7	7.22	m	127.6	7.21	m	127.6	7.21	m	127.6
Ala	NMe	2.72	s	31.4	2.72	s	31.6	2.72	s	31.6
	1			172.5			172.7			172.7
	2	5.32	q, 6.6	50.9	5.32	q, 6.6	50.9	5.32	q, 6.6	50.9
Val1	3	1.03	d, 6.6	14.1	1.04	d, 6.6	14.1	10.3	d, 6.6	14.2
	NMe	2.09	s	29.9	2.10	s	30.0	2.09	s	29.8
	1			171.6			171.6			171.7
Val1	2	4.42	dd, 4.8, 8.8	54.3	4.43	dd, 4.8, 8.8	54.3	4.42	dd, 4.8, 8.8	54.3
	3	1.63	m	31.6	1.64	m	31.5	1.63	m	31.5
	4	0.69	d, 7.0	17.1	0.69	d, 7.0	17.2	0.69	d, 7.0	17.2
	5	0.82	d, 7.0	19.9	0.82	d, 7.0	20.0	0.82	d, 7.0	20.0
	NH	6.58	bd, 8.8		6.58	bd, 8.8		6.57	bd, 8.8	
	1			170.4			170.5			170.4
Val2	2	4.53	d, 11.0	63.4	4.53	d, 11.0	63.5	4.53	d, 11.0	63.5
	3	2.16	m	26.8	2.16	m	26.8	2.17	m	26.8
	4	0.69	d, 7.0	18.8	0.69	d, 7.0	18.9	0.69	d, 7.0	18.9
	5	0.82	d, 7.0	20.6	0.82	d, 7.0	20.6	0.82	d, 7.0	20.6
	NMe	2.91	s	31.1	2.92	s	31.2	2.91	s	31.2
	1			172.6			173.0			172.7
Val3	2	5.15	d, 10.6	59.1	5.16	d, 10.6	59.2	5.16	d, 10.6	59.2
	3	2.30	m	27.7	2.30	m	27.8	2.29	m	27.8
	4	0.77	d, 6.6	18.7	0.79	d, 6.6	18.9	0.78	d, 6.6	18.8
	5	0.89	d, 6.2	20.3	0.89	d, 6.2	20.4	0.89	d, 6.2	20.4
	NMe	2.88	s	30.7	2.88	s	30.8	2.88	s	30.8
	1			177.4			177.5			177.6
lipid	2	2.76	m	36.6	2.77	m	36.7	2.76	m	36.7
	3	1.28, 1.64	m, m	34.5	1.32, 1.68	m, m	34.3	1.30, 1.66	m, m	34.6
	4	1.20	dt, 7.3, 14.8	27.8	1.32	m	27.5	1.26	m	27.8
	5	1.47	dt, 7.5, 14.8	24.5	1.45	dt, 7.5, 14.8	29.4	1.36	m	27.7
	6	2.38	t, 7.5	43.8	2.14	m	18.8	2.02	dt, 7.3, 7.0	34.5
	7			209.6			85.5	5.81	m	140.1
	8	2.04	s	30.0	n/o ^c		69.8	4.91, 4.98	dd, dd	115.0
	9	0.99	d, 6.6	18.4	1.00	d, 6.6	18.5	1.00	d, 6.6	18.5

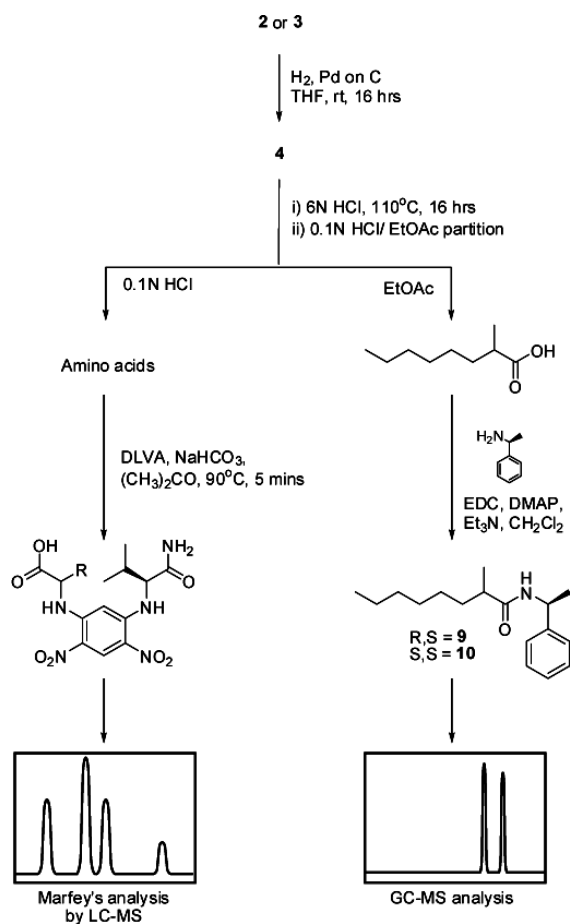
^a Recorded at 400 MHz. ^b Recorded at 100 MHz. ^c n/o = not observed.

with *N*_α-(2,4-dinitro-5-fluorophenyl)-L-valinamide (DLVA) under standard conditions and analyzed by gradient C₁₈ RP-HPLC in each case. Comparison of the retention times and mass spectra for these derivatives with commercially available standards derivatized under identical conditions allowed assignment of all amino acid residues as L for almiramides A–C. These assignments were subsequently confirmed by co-injection analyses. The lipid chains of **2** and **3** from the organic phases of the hydrolysis reactions were separately derivatized with (*S*)-1-phenylethylamine under standard amide coupling conditions (Scheme 1) to form compound **9**. Commercially available (±)-2-methyloctanoic acid was similarly derivatized to give compounds **9** and **10**, which were separated by flash silica gel column chromatography. Stereoidentification of these two products was accomplished by X-ray analysis of compound **9**, which defined the structure as (2*R*)-2-methyl-*N*-((*S*)-1-phenylethyl)octanamide. Comparison of the GC retention times of these synthetic materials by GC analysis with that of the natural product derived fragments showed that both **2** and **3** possessed 2-*R* configurations. Comparison of the NMR chemical shifts for **1**, **2**, and **3**, and consideration of the common biosynthetic origin of these

three compounds, makes it highly likely that this center in compound **1** is also *R*, although this was not verified experimentally.

This result was somewhat surprising because a recent total synthesis of the related metabolite dragonamide A (**5**) has shown it to contain the opposite (2*S*)-2-methyloct-7-ynoic acid moiety.¹⁰ Work from the Panama ICBG has provided evidence that another related metabolite, dragonamide B (**6**), also contains the (2*S*)-2-methyloct-7-ynoic acid subunit.¹¹ Fortunately, compound **6** was also isolated as a component of an inactive fraction from the crude extract investigated in this study. We therefore analyzed an authentic sample of **6** under identical conditions. GC–MS analysis indicated that (2*S*)-2-methyl-*N*-((*S*)-1-phenylethyl)octanamide (**10**) was produced as the sole product from **6**, in line with previous reports for this class of compounds.

Thus, this strain of *L. majuscula* possesses the biosynthetic capability to produce two closely related compounds (**2** and **6**) that contain constitutively identical lipid chains with opposite configurations. A recent study of enoylreductases (ER) in modular type I polyketide synthases has shown that the presence or absence of a single tyrosine residue in the active

Scheme 1. Configurational Analysis Strategy for **2** and **3**

site of the ER domain defines the configuration of the final methyl-branched product as *R* or *S* for all systems in which a propionate unit is incorporated to form the branched methyl substituent.¹² Using site-directed mutagenesis, the authors were able to validate this hypothesis by generating mutants that produced compounds bearing opposite configurations at these positions by replacement or insertion of this key tyrosine residue. Although pendent methyl groups in cyanobacterial natural products originate from *S*-adenosyl methionine (SAM) rather than incorporation of propionate subunits,¹³ both of these biosynthetic pathways proceed via a common α,β unsaturated carbonyl species, which is reduced by the ER module to form the saturated final product. It is therefore likely that this organism contains separate PKS-NRPS clusters for the production of the almiramide versus the dragonamide series and that differences within the ER modules of these two clusters give rise to the observed configurational differences in the two alkyl side chains.

Biological evaluation of these three compounds showed that compounds **2** and **3** possessed strong *in vitro* antiparasitic activity against *L. donovani* (IC_{50} = 2.4 and 1.9 μM , respectively), whereas compound **1** was completely inactive up to 13.5 μM , thus indicating the requirement of an unsaturated terminus on the side chain for activity. For reference, the two most widely used treatments against leishmaniasis (sodium stibogluconate and miltefosine) are active *in vitro* against *L. donovani* with IC_{50} values of 44.7 and 0.5 μM , respectively. Previous investigations of cyanobacteria from the Caribbean by our groups have provided a number of related secondary metabolites including carmabin A (**7**),

dragomabin (**8**), and dragonamides A (**5**) and B (**6**).¹¹ Parallel testing with almiramides A–C showed compounds **5**–**8** to be inactive up to the highest tested concentrations (10 $\mu\text{g}/\text{mL}$), despite significant structural similarities between these compounds and almiramides B and C (Figure 2). These data suggest that **2** and **3** are highly specific for *L. donovani* and that possession of alkyne and primary amide termini for *N*-methylated peptides is insufficient for activity against this organism. Almiramides A–C (**1**–**3**) were also tested for activity against both *Plasmodium falciparum* (W2 chloroquine-resistant strain) and *Trypanosoma cruzi* and found to be inactive up to the highest tested concentrations (13.5 μM) in all cases.

The value of the almiramides as lead molecules for antileishmanial drug development prompted us to further explore the SAR features of these compounds by the generation of semisynthetic analogues. Hydrogenation of **2** with H_2 and 10% palladium on carbon afforded compound **4** in quantitative yield. Evaluation of **4** in the leishmaniasis assay showed it to be inactive at the highest tested concentration (13.4 μM), supporting the hypothesis that the unsaturated terminus plays an important role in the interaction of these compounds with their biological target. We next explored the importance of the primary and secondary amides for activity in the almiramide series. Methylation of **2** with NaH/MeI afforded a 1:1 mixture of compounds **11** and **12** (Scheme 2), which exhibited IC_{50} values of 1.64 and 2.31 μM , respectively. We hypothesize that the improved activity of **11** over **2** is due to its increased membrane permeability. Indeed, there have been a number of studies that recognize the importance of methylation patterns in determining the degree of membrane permeability for both cyclic and linear peptidic small molecules,^{14,15} which is in line with our observed results.

The small quantities of **11** and **12** generated from derivatization of the natural product precluded the use of standard techniques for their structural characterization. Unequivocal assignment of their structures was possible by consideration of a combination of ^1H NMR and MS fragmentation data. ^1H NMR for **11** showed the absence of the Val1-NH proton doublet at δ 6.58 and the presence of a new methyl singlet at δ 2.94. Coupled with a mass increase of 14 amu in the HRESIMS, this strongly suggested that the Val1-NH proton in **2** had been replaced with a methyl group in **11**. This was confirmed by consideration of the HRESIMS fragmentation pattern that showed characteristic fragments for the loss of sequential amino acid residues starting from the C-terminus and placed the new methyl group on residue Val1 (Supporting Information). Similarly, ^1H NMR for **12** showed the absence of both the Val1-NH and the C-terminal-NH₂ proton resonances (δ 6.58, δ 5.80, and δ 6.26) and the presence of three additional methyl singlets in the region δ 2.84–2.94 indicating a permethylation product. As with compound **11**, this was confirmed by the MS fragmentation pattern in the HRESIMS spectrum, which indicated methylation of residue Val1 and dimethylation of the phenylalanine residue (Supporting Information). Interestingly the permethylated compound **12** displayed a single conformation on the NMR time scale, in contrast to compounds **1**–**4** and **11**, which all exhibited major and minor conformers in their NMR spectra.¹⁶ This suggests that the C-terminal-NH protons play an important role in hydrogen bonding interactions which leads to these two conformational states.

Generation of semisynthetic derivatives with fully methylated peptide backbones and improved selectivity indices was particularly encouraging, as this opened the door to a facile

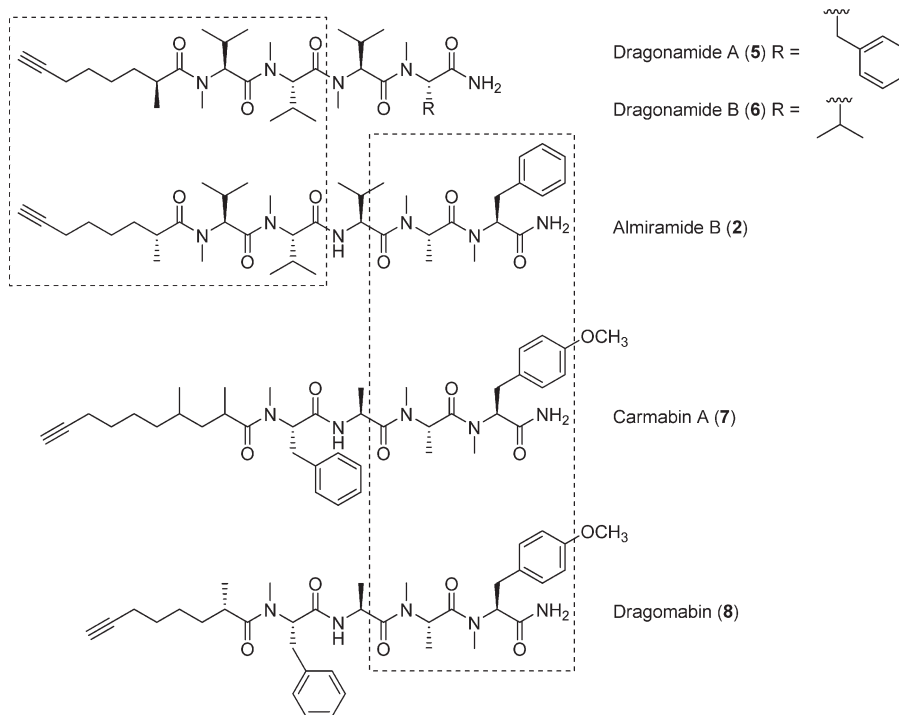
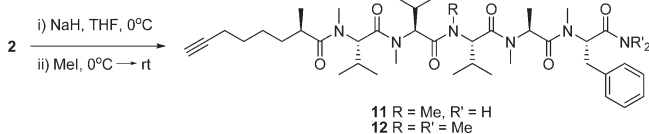


Figure 2. Structurally related linear lipopeptides (areas of structural homology outlined with dashed lines).

Scheme 2. Generation of Semisynthetic Derivatives **11** and **12**



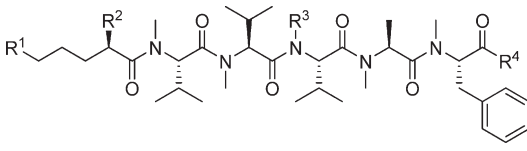
synthetic route for the generation of peptide libraries and the production of large quantities of material for further *in vitro* and *in vivo* testing. We therefore elected to undertake the synthesis of a small library of simplified synthetic analogues (**13–24**) to probe the viability of this scaffold as a lead for future medicinal chemistry and drug development. In designing this initial library, we were motivated to explore the SAR attributes of both the C and N termini in the hope of finding a suitable synthetic analogue from which to launch the construction of larger, more complex combinatorial libraries. Fortunately, the peptidic nature of these compounds makes them amenable to solid phase peptide synthesis (SPPS) to construct the core framework. This approach permits a divergent strategy by which different solid supports can be employed to generate a variety of functional groups at the C-terminus, and addition of the unsaturated alkyl chain as the final step on the solid support provides access to structural diversity at the N-terminus. The library was designed in such a way that the closest analogue (**13**) differed from **12** only in the absence of the methyl group at the α -position of the lipophilic side chain, while additional library members showed incrementally greater structural divergence.

In brief, the linear pentapeptide precursor was constructed using standard SPPS techniques starting from either Rink amide or chlorotrityl resins. Addition of the appropriate alkyl chain to the pentapeptide by formation of the corresponding amide bond using HBTU and diisopropylethylamine (DIPEA) was followed by cleavage from the solid support (1% TFA in CH_2Cl_2 for chlorotrityl resins, 95% TFA, 5%

TIPS for Rink amide resins). The resulting intermediates were permethylated with NaH/MeI in THF under argon, and the reactions were monitored by LC–MS. In all cases, final purification was performed by RP–HPLC (Phenomenex Jupiter C₁₈ column, 4.6 mm \times 250 mm, 1 mL/min, MeOH/H₂O + 0.02% HCOOH). Conversion of compounds **17–20** to their corresponding methyl esters (**21–24**) was accomplished by treatment with TMS-diazomethane.

Biological evaluation of compounds **13–24** in parallel with the original lead compounds (**1–3**) identified several new structures with comparable activities to the original natural products (Table 2). Specifically, compounds **13–16** containing the *N,N*-dimethylamide C-terminus exhibited strong antileishmanial activities. By contrast, the corresponding methyl ester derivatives (**21–24**) were completely inactive in this screen, and the carboxylic acid derivatives (**17–20**) showed mixed activities. In addition to screening for antileishmanial activities, compounds **13–24** were also evaluated for their cytotoxic properties. Using a standard screening protocol against mammalian Vero cells, we were able to demonstrate that several of these synthetic analogues possessed improved toxicity profiles compared with the natural products. Compound **15** showed particular promise in this regard, with activity against *L. donovani* of 3.1 μM (IC₅₀) and a cytotoxicity to Vero cells of 155.7 μM , giving this compound a 50-fold selectivity index. Given that these initial library members display potencies that are close to those of the best currently available therapeutics (e.g., miltefosine potency of 0.5 μM) and that the therapeutic indices are encouraging, we therefore consider these compounds promising lead candidates for further development. Synthesis of second generation libraries is currently ongoing in our laboratory.

The synthesis of compounds **13–16**, which exhibit improved selectivity profiles over the initial natural product lead structures, is an important finding for two reasons. First, this discovery circumvents one of the most common impediments to the development of natural product drug leads by providing

Table 2. Structure and Bioactivities of Almiramide A–C and Synthetic Derivatives^a


Compound	R ¹	R ²	R ³	R ⁴	Bioactivity (IC ₅₀ , μM)		
					<i>Leishmania donovani</i>	Cytotoxicity (Vero cells)	Selectivity Index
1		Me	H	NH ₂	>13.5	113.1	-
2		Me	H	NH ₂	2.4	52.3	21.8
3		Me	H	NH ₂	1.9	33.1	17.4
4		Me	H	NH ₂	>13.7	nt	-
11		Me	Me	NH ₂	1.6	nt	-
12		Me	Me	NMe ₂	2.3	nt	-
13		H	Me	NMe ₂	5.9	159.4	27.0
14		H	Me	NMe ₂	2.7	23.8	8.8
15		H	Me	NMe ₂	3.1	155.7	50.2
16		H	Me	NMe ₂	6.7	93.1	13.9
17		H	Me	OH	>14.0	> 68.9	-
18		H	Me	OH	4.1	192.4	46.9
19		H	Me	OH	5.6	281.1	50.2
20		H	Me	OH	>14.0	> 70.0	-
21		H	Me	OMe	>14.0	27.0	-
22		H	Me	OMe	>14.0	18.8	-
23		H	Me	OMe	>14.0	41.4	-
24		H	Me	OMe	>14.0	24.7	-

^a nt = not tested.

an efficient route to a renewable supply of material, an essential requirement for preliminary in vivo studies that typically requires more material than is available from the natural source. Second, the peptidic nature of this scaffold makes it an ideal candidate for the construction of targeted combinatorial libraries. However, the presence of a standard (nonmethylated) residue at Val1 and a chiral center at C-2 of the aglycone makes the large scale synthesis of the natural product a comparatively laborious process. By demonstrating that structural variations are tolerated at these positions, we have been able to design an efficient route to a simplified family of synthetic analogues that not only proceeds in high yield but also provides the opportunity to explore the SAR interdependence of the amino acid residues present in this framework. For reference, the recent total synthesis of dragonamide A (**5**) required 17 steps in the longest linear sequence starting from 1,5-pentanediol. By contrast, the synthesis of **17** was completed in just 1 day, with all but two of the steps performed on the solid phase.

Conclusion

We have identified a novel family of cyanobacterial natural products with in vitro activity against the protozoan parasite *Leishmania donovani*. Structure elucidation and configurational determination were accomplished using a combination of analytical and degradative techniques and revealed the presence of the (2*R*)-methyloct-7-ynoic acid lipid terminus, in contrast to the (2*S*)-methyloct-7-ynoic acid terminus found in the related compounds dragonamides A (**5**) and B (**6**). Synthesis of a small library of related structures has identified compounds with similar potencies against *L. donovani* and superior cytotoxicity profiles. These new compounds can be efficiently synthesized using SPPS methodology and provide incentive for the initiation of a drug development program based on these lead structures.

Experimental Section

General Experimental Procedures. NMR spectra were acquired on 400, 500, and 600 MHz spectrometers equipped with

5 mm inverse detection probe, 5 mm broadband probe, and 5 mm HCN triple resonance cryoprobe, respectively, and referenced to residual solvent proton and carbon signals (δ_{H} 1.94, δ_{C} 1.34 for CD_3CN and δ_{H} 3.31, δ_{C} 49.15 for CD_3OD). HPLC purifications were performed with a Phenomenex Jupiter C_{18} (4.6 mm \times 250 mm, 5 μm) RP-HPLC column unless otherwise stated. All solvents were HPLC grade and were used without further purification. HPLC analysis data were obtained for all compounds, and purity over 95% was confirmed for all synthesized compounds.

Collection. The cyanobacterium *Lyngbya majuscula* (46.5 g dry wt) was collected by hand from a depth of 0.1–0.3 m from mangrove roots on a small island in the Bocas del Toro National Marine Park, Bocas del Toro Province on the north coast of Panama (09° 16.669' N, 82° 09.834' W). The cyanobacterium was strained through a mesh bag to remove excess seawater, frozen on site, and stored at -4°C until workup. The taxonomy was identified by comparison with characteristics described by Geitler.¹⁷ A voucher was deposited at the Smithsonian Tropical Research Institute, Panama (voucher number PAB-04-NOV-05-7).

Extraction and Isolation. Freshly thawed material was extracted exhaustively with $\text{CH}_2\text{Cl}_2/\text{MeOH}$ (2:1, 3 \times 500 mL) and the combined organic extracts were partitioned against H_2O (200 mL) and concentrated to dryness in vacuo to give 0.57 g of a dark-brown gum. This material was subjected to flash Si gel CC (Aldrich, Si gel 60, 230–400 mesh, 40 mm \times 180 mm) eluting with 100% hexanes (300 mL), 9:1 hexanes/EtOAc (300 mL), 8:2 hexanes/EtOAc (300 mL), 6:4 hexanes/EtOAc (300 mL), 4:6 hexanes/EtOAc (300 mL), 2:8 hexanes/EtOAc (300 mL), 100% EtOAc (300 mL), 3:1 EtOAc/MeOH (300 mL), 100% MeOH (300 mL). Two contiguous fractions (100% EtOAc, 3:1 EtOAc/MeOH) showed antileishmanial activity and possessed similar LC-MS and NMR features. These were separately subjected to C_{18} RP-SPE chromatography, eluting with 1:1 $\text{H}_2\text{O}/\text{MeOH}$ (30 mL), 4:6 $\text{H}_2\text{O}/\text{MeOH}$ (30 mL), 3:7 $\text{H}_2\text{O}/\text{MeOH}$ (30 mL), 2:8 $\text{H}_2\text{O}/\text{MeOH}$ (30 mL), 1:9 $\text{H}_2\text{O}/\text{MeOH}$ (30 mL), 100% MeOH (30 mL), 100% EtOAc (30 mL). The active 3:7 $\text{H}_2\text{O}/\text{MeOH}$ fraction was subjected to C_{18} RP-HPLC (57% MeOH/43% H_2O , 210 nm, 1 mL/min) to give almiramide A (**1**) as a colorless glass (3.5 mg, 0.6% of crude extract, $t_{\text{R}} = 15.4$ min) and almiramide B (**2**) as a colorless glass (1.9 mg, 0.3% of crude extract, $t_{\text{R}} = 39.1$ min). HPLC of the 2:8 $\text{H}_2\text{O}/\text{MeOH}$ active fraction (62% MeOH/38% H_2O , 210 nm, 1 mL/min) gave almiramide B (**2**) as a colorless glass (3.4 mg, 0.6% of crude extract, $t_{\text{R}} = 16.9$ min) and almiramide C (**3**) as a colorless glass (1.2 mg, 0.2% of crude extract, $t_{\text{R}} = 40.3$ min).

Purification of the 100% EtOAc fraction from the original normal phase fractionation by C_{18} RP-HPLC (Prontosil 120-5- C_{18} 4.6 mm \times 150 mm RP-HPLC column, 5 μm , 64% MeOH/34% H_2O , 210 nm, 1 mL/min) afforded dragonamide B (**6**) as a colorless glass (1.1 mg, 0.2% of crude extract, $t_{\text{R}} = 27.1$ min) which was identical to previously isolated material by ^1H and ^{13}C NMR spectroscopy and APCI mass spectrometry.

Almiramide A (1): colorless glass; $[\alpha]_{\text{D}}^{22} -169.1$ (c 0.2, MeOH); UV (MeOH) λ_{max} (log ϵ) 228 (sh) (3.77) nm; IR (film) ν_{max} 2960, 1624 cm^{-1} ; for ^1H and ^{13}C NMR data, see Table 1; APCIMS m/z 743.3 $[\text{M} + \text{H}]^+$ (35), 565.4 (39), 381.3 (100), 268.2 (27); HRESIMS m/z $[\text{M} + \text{H}]^+$ 743.5062 (calcd for $\text{C}_{40}\text{H}_{67}\text{N}_6\text{O}_7$, 743.5065).

Almiramide B (2): colorless glass; $[\alpha]_{\text{D}}^{22} -148.9$ (c 0.1, MeOH); UV (MeOH) λ_{max} (log ϵ) 230 (sh) (3.76) nm; IR (film) ν_{max} 2970, 1634 cm^{-1} ; for ^1H and ^{13}C NMR data, see Table 1; APCIMS m/z 727.4 $[\text{M} + \text{H}]^+$ (37), 549.4 (63), 365.3 (100), 252.2 (45); HRESIMS m/z $[\text{M} + \text{H}]^+$ 725.4964 (calcd for $\text{C}_{40}\text{H}_{65}\text{N}_6\text{O}_6$, 725.4960).

Almiramide C (3): colorless glass; $[\alpha]_{\text{D}}^{22} -136.8$ (c 0.1, MeOH); UV (MeOH) λ_{max} (log ϵ) 228 (sh) (3.69) nm; IR (film) ν_{max} 2955, 1630 cm^{-1} ; for ^1H and ^{13}C NMR data, see Table 1; APCIMS m/z 725.4 $[\text{M} + \text{H}]^+$ (33), 547.4 (67), 363.3 (100), 250.2

(43); HRESIMS m/z $[\text{M} + \text{H}]^+$ 727.5115 (calcd for $\text{C}_{40}\text{H}_{67}\text{N}_6\text{O}_6$, 727.5116).

Hydrogenation of 2 and 3. Authentic samples of **2** and **3** (0.1 mg) were independently dissolved in dry CH_2Cl_2 (10 mL). Then 10% palladium on carbon (2 mg) was added and the suspensions were stirred under an atmosphere of H_2 (balloon) at room temperature for 16 h. Each sample was concentrated to dryness under a stream of N_2 , dissolved in MeOH (1 mL), and filtered through a 13 mm 0.2 μm nylon filter. The resulting filtrates were concentrated to dryness under a stream of N_2 and purified by C_{18} RP-HPLC (76% MeOH/24% H_2O , 210 nm, 1 mL/min) to give **4** as a white solid (0.1 mg, >99% yield) in each case.

Tetrahydroalmiramide B (4): white solid; $[\alpha]_{\text{D}}^{20} -160$ (c 0.013, CH_3OH); UV (MeOH) λ_{max} (log ϵ) 219 (sh) (4.09) nm; IR (NaCl, cm^{-1}) ν_{max} 3400, 2925, 2855, 1731, 1643, 1463 cm^{-1} ; ^1H NMR (CD_3OD , 600 MHz) δ 7.31–7.28 (m, 2H), 7.27–7.24 (m, 3H), 5.55 (dd, $J = 12.6, 4.8$ Hz, 1H), 5.40 (bd, $J = 6.6$ Hz, 1H), 5.20 (d, $J = 10.8$ Hz, 1H), 4.60–4.59 (m, 1H), 4.40 (d, $J = 6.6$ Hz, 1H), 3.66–3.62 (m, 3H), 3.43–3.40 (m, 1H), 3.19–3.18 (m, 1H), 3.05 (s, 3H), 3.00 (s, 3H), 2.84 (s, 3H), 2.36–2.29 (m, 5H), 2.18 (s, 3H), 2.04–2.00 (m, 5H), 1.64–1.57 (m, 2H), 1.09 (d, $J = 6.6$ Hz, 2H), 1.06 (d, $J = 6.6$ Hz, 2H), 0.92–0.82 (m, 13H), 0.81–0.74 (m, 6H); HRESIMS m/z $[\text{M} + \text{Na}]^+$ 751.5085 (calcd for $\text{C}_{40}\text{H}_{68}\text{N}_6\text{O}_6\text{Na}$, 751.5093).

Marfey's Analysis of 1–3. An authentic sample of **1** and hydrogenated samples of **2** and **3** were independently treated with 6 N HCl in sealed vials at 120°C for 18 h. The solutions were concentrated to dryness in vacuo and treated with a solution of 1-fluoro-2,4-dinitrophenyl-5-L-valineamide (DLVA) (0.25 mg, 0.8 μmol) in acetone (50 μL) and a solution of 0.1 M NaHCO_3 (100 μL) in a sealed vial at 90°C for 5 min. The reaction mixture was neutralized with 2 N HCl (50 μL) and diluted with CH_3CN (100 μL). The resulting solution was analyzed by C_{18} RP-HPLC employing a Phenomenex Jupiter C_{18} column (4.6 mm \times 250 mm) and a gradient elution profile of 25% $\text{CH}_3\text{CN}/75\%$ H_2O (acidified with 0.05% HCOOH) to 55% $\text{CH}_3\text{CN}/45\%$ H_2O (acidified with 0.05% HCOOH) over 60 min at a flow of 0.5 mL/min, monitoring at 340 nm. Retention times in minutes for the derivatized amino acid standards were as follows: L-N-methylalanine 32.2; D-N-methylalanine 32.9; L-valine 35.7; L-N-methylvaline 42.3; L-N-methylphenylalanine 45.7; D-valine and D-N-methylphenylalanine 47.8; D-N-methylvaline 50.3.

Synthesis of 9 and 10. To a stirred solution of (\pm)-2-methyloctanoic acid (82 mg, 0.52 mmol) in dry CH_2Cl_2 (10 mL) at 0°C was added (*S*)-1-phenylethylamine (65 μL , 0.57 mmol), Et_3N (57 μL , 0.78 mmol, freshly distilled over CaH), 1-ethyl-3-(3-dimethylaminopropyl)carbodiimide (109.4 mg, 0.57 mmol), and 4-di(methylamino)pyridine (6 mg, 0.05 mmol). The reaction mixture was allowed to warm to room temperature and stirred for 18 h. The volatiles were removed in vacuo, and the residue was suspended in EtOAc (5 mL) and filtered through Celite. The filtrate was diluted with EtOAc (10 mL) and washed sequentially with 0.2 N HCl (25 mL), H_2O (25 mL), 0.1 N NaHCO_3 (25 mL), and H_2O (25 mL) and concentrated to dryness in vacuo to give a white crystalline solid. This material was purified by two steps of flash silica gel column chromatography (26 mm \times 250 mm, 100% hexanes to 7:3 hexanes/EtOAc; 14 mm \times 210 mm, 85:15 hexanes/EtOAc) to give compounds **9** (33 mg, 24%) and **10** (38.4 mg, 28%) as an optically active crystalline white solid and an optically active colorless glass respectively.

(2*R*)-2-Methyl-N-((*S*)-1-phenylethyl)octanamide (9): white needles ($^i\text{PrOH}$); $[\alpha]_{\text{D}}^{20} -85.3$ (c 0.13, CHCl_3); UV (MeOH) λ_{max} (log ϵ) 214 (3.71) nm; IR (NaCl, cm^{-1}) ν_{max} 3298, 2966, 2921, 2851, 1639, 1546 cm^{-1} ; ^1H NMR (CDCl_3 , 300 MHz) δ 7.28–7.16 (5H, m), 5.62 (1H, bd, $J = 7.8$ Hz), 5.09 (1H, dq, $J = 7.3, 7.3$ Hz), 2.08 (1H, m), 1.59 (1H, m), 1.43 (3H, d, $J = 6.9$ Hz), 1.33–1.14 (9H, m), 1.05 (3H, d, $J = 6.8$ Hz), 0.82 (3H, t, $J = 6.7$ Hz); ^{13}C NMR (CDCl_3 , 75 MHz) δ 175.5, 128.6, 127.3, 126.1, 48.3, 41.7, 34.4, 31.7, 29.3, 27.4, 22.6, 21.7, 17.8, 14.0;

HRESIMS m/z [M + H]⁺ 262.2171 (calcd for C₁₇H₂₈NO, 262.2165).

(2S)-2-Methyl-N-((S)-1-phenylethyl)octanamide (10): colorless glass; $[\alpha]_D^{20}$ -66.1 (*c* 0.14, CHCl₃); UV (MeOH) λ_{\max} (log ϵ) 215 (3.71) nm; IR (NaCl, cm⁻¹) ν_{\max} 3304, 2961, 2928, 2853, 1640, 1540 cm⁻¹; ¹H NMR (CDCl₃, 600 MHz) δ 7.33–7.24 (5H, m), 5.57 (1H, bd, *J* = 7.8 Hz), 5.12 (1H, q, *J* = 7.2 Hz), 2.11 (1H, m), 1.59 (1H, m), 1.47 (3H, d, *J* = 6.6 Hz), 1.34 (1H, m), 1.24–1.19 (9H, m), 1.12 (3H, d, *J* = 6.6 Hz), 0.83 (3H, t, *J* = 6.6 Hz); ¹³C NMR (CDCl₃, 75 MHz) δ 175.6, 128.6, 127.2, 126.1, 48.3, 41.6, 34.4, 31.7, 29.2, 27.4, 22.5, 21.6, 17.8, 14.0; HRESIMS m/z [M + H]⁺ 262.2173 (calcd for C₁₇H₂₈NO, 262.2165).

GC–MS Analysis of 9 and 10. GC–MS analyses were performed on an Altech Chirasil Val column (25 m × 0.25 mm, 0.16 μ m i.d.) employing a temperature gradient from 90 to 220 °C at a ramp rate of 4 °C/min followed by 5 min at 220 °C. Retention times in minutes for compounds **9** and **10** were as follows: **9** 25.61, **10** 25.05.

Methylation of 2. To a stirred solution of **2** (2 mg, 0.002 mmol) in dry THF (1 mL) was added NaH (60% dispersion in oil, 2 mg, 0.05 mmol), and the solution was stirred under argon at room temperature for 2 h. MeI (50 μ L, 0.80 mmol) was added dropwise and the resulting solution stirred for a further 21 h. The reaction mixture was quenched with water (0.5 mL) and partitioned with EtOAc (2 mL). The phases were separated, and the aqueous phase was washed with EtOAc (2 mL). The combined organics were concentrated to dryness under a stream of N₂ gas and purified by C₁₈ RP-HPLC (72% MeOH/28% H₂O, 210 nm, 0.8 mL/min) to give **11** (0.2 mg, 13%) and **12** (0.6 mg, 38%) as white solids.

Monomethylalmiramide B (11): white amorphous solid; $[\alpha]_D^{22}$ -80 (*c* 0.03, MeOH); UV (MeOH) λ_{\max} (log ϵ) 228 (3.77) nm; IR (NaCl) ν_{\max} 3400, 2926, 1634, 1463 cm⁻¹; ¹H NMR (CD₃CN, 600 MHz) δ 7.30–7.28 (m, 2H), 7.23–7.21 (m, 3H), 5.39–5.36 (m, 2H), 5.16 (d, *J* = 10.8 Hz, 1H), 5.08 (d, *J* = 10.8 Hz, 1H), 4.80 (d, *J* = 10.8 Hz, 1H), 3.29 (dd, *J* = 15, 4.8 Hz, 1H), 2.93 (s, 3H), 2.92 (s, 3H), 2.84 (s, 3H), 2.75 (s, 3H), 2.29–2.21 (m, 3H), 2.10 (s, 3H), 1.46 (q, *J* = 7.2 Hz, 2H), 1.35–1.28 (m, 4H), 1.00 (d, *J* = 6.6 Hz, 7H), 0.84–0.81 (m, 8H), 0.77 (d, *J* = 6.6 Hz, 5H), 0.76 (d, *J* = 6.6 Hz, 3H), 0.69 (dd, *J* = 6.6, 2.4 Hz, 7H); HRESIMS m/z [M + Na]⁺ 761.4938 (calcd for C₄₁H₆₆N₆O₆Na, 761.4936).

Permethyalmiramide B (12): white amorphous solid; $[\alpha]_D^{22}$ -240 (*c* 0.08, MeOH); UV (MeOH) λ_{\max} (log ϵ) 225 (sh) (3.93) nm; IR (NaCl) ν_{\max} 3400, 2962, 2929, 1637, 1463, 1401 cm⁻¹; ¹H NMR (CD₃CN, 600 MHz) δ 7.27 (t, *J* = 7.8 Hz, 2H), 7.24 (d, *J* = 6.6 Hz, 2H), 7.19 (t, *J* = 7.2 Hz, 1H), 5.75 (dd, *J* = 9.6, 6.6 Hz, 1H), 5.39 (q, *J* = 13.2, 6.6 Hz, 1H), 5.16 (d, *J* = 10.8 Hz, 1H), 5.09 (d, *J* = 10.8 Hz, 1H), 4.91 (d, *J* = 10.8 Hz, 1H), 3.07 (dd, *J* = 14.4, 6 Hz, 1H), 2.93 (s, 3H), 2.92 (s, 6H), 2.86 (s, 3H), 2.84 (s, 3H), 2.83 (s, 3H), 2.28–2.22 (m, 3H), 2.21 (s, 3H), 1.46 (q, *J* = 6.6 Hz, 2H), 1.35–1.27 (m, 3H), 1.00 (dd, *J* = 6.6, 4.2 Hz, 6H), 0.84 (t, *J* = 7.2 Hz, 6H), 0.78 (t, *J* = 6.6 Hz, 6H), 0.70 (t, *J* = 6.6 Hz, 6H); ¹³C NMR (CD₃OD, 125 MHz) δ 14.6, 18.4, 18.5, 19.0, 19.1, 19.7, 20.4, 27.9, 28.4, 28.6, 29.8, 30.4, 31.1, 31.2, 31.3, 34.7, 35.3, 36.1, 36.3, 37.5, 37.8, 51.5, 55.7, 59.8, 59.9, 60.0, 69.7, 84.9, 128.1, 129.7, 130.6, 138.6, 170.6, 171.8, 172.0, 172.6, 172.7, 179.6; HRESIMS m/z [M + Na]⁺ 789.5258 (calcd for C₄₃H₇₀N₆O₆Na, 789.5249).

Bioassays. All bioassays were performed in duplicate, testing at 10, 2, 0.4, 0.08, and 0.016 μ g/mL. Malaria bioassays were performed as previously reported by our program, using chloroquine as a positive control (IC₅₀ = 80–100 nM).¹⁸ Chagas bioassays were performed following the protocol of Buckner et al. and using nifurtimox as a positive control (IC₅₀ = 3–5 μ g/mL).¹⁹ Leishmaniasis bioassays were performed using a method previously employed in our laboratory, based on parasite DNA fluorescence.²⁰ In this latter assay, amphotericin B was used as the positive control and had an IC₅₀ of 80 ng/mL.

Cytotoxicity bioassays were performed following an 3-[4,5-dimethylthiazol-2-yl]-2,5-diphenyltetrazolium bromide (MTT) cell proliferation assay protocol with green monkey Vero kidney cells.

Representative Library Member Synthesis. Fmoc-L-phenylalanine (3.246 g, 8.37 mmol) and DIPEA (2.7 mL, 16.7 mmol) were added to a stirred suspension of 2-chlorotriethyl chloride resin (1.047 g, 200–400 mesh, 1% DBV) in dichloromethane (50 mL) under argon, and the resulting suspension was stirred at room temperature for 3 h. The solution was transferred to a polypropylene vessel containing a fritted disk and fitted with a Teflon stopcock, drained, and washed (3 × 20 mL of CH₂Cl₂, 3 × 20 mL of DMF, 3 × 20 mL of CH₂Cl₂). The resulting pale-yellow resin was air-dried for 24 h and analyzed to determine the loading value of the phenylalanine substrate as outlined below.

Two aliquots (7.5 mg and 6.6 mg) of the resin were transferred to Eppendorf tubes, dissolved in 1% DBU in DMF (500 μ L), and agitated for 1 h. Then 50 μ L aliquots of these solutions were diluted with DMF (6 mL), and absorbance was measured at λ = 301 nm to determine the loading value of the Fmoc-L-phenylalanine as 2.56 mmol per gram of resin.

Subsequent amino acids were added using a standard protocol. The dried resin was allowed to swell for 5 min in CH₂Cl₂ (10 mL), drained, and washed with DMF (10 mL). The washed resin was deprotected using 20% piperidine in DMF (20 mL) with agitation for 20 min. After deprotection, the resin was drained and washed (3 × 20 mL of DMF, 3 × 20 mL of CH₂Cl₂, 3 × 20 mL of DMF). To this washed resin was added a solution of HBTU (4.983 g, 13.1 mmol), the appropriate amino acid (13.4 mmol), and DIPEA (4.4 mL, 26.8 mmol). The resulting suspension was gently agitated for 1 h, drained, and washed, as described above. This process was repeated with successive amino acids as appropriate to form resin-bound Phe-Ala-Val-Val-Fmoc.

From this common pentapeptide precursor, library members were synthesized by addition of appropriate alkyl acids. For compound **22**, loaded resin (82.5 mg) was deprotected by treatment with 20% piperidine in DMF (5 mL) with agitation for 20 min. 7-Octenoic acid (32 μ L, 0.21 mmol), HBTU (77.4 mg, 0.20 mmol), and DIPEA (70 μ L, 0.42 mmol) were added, and the resulting suspension was agitated for 1 h, drained, and washed as previously described. The resulting linear lipopeptide was cleaved from the resin by treatment with 1% TFA in CH₂Cl₂ for 20 min and the solvent removed by evaporation under a stream of N₂ gas. The resulting glossy white solid was triturated with *tert*-butyl methyl ether and centrifuged at 1000 rpm for 20 min. Removal of the *tert*-butyl methyl ether afforded the lipopeptide as a white solid (12.7 mg) which was carried to the next step without further purification. To a solution of this lipopeptide in THF (10 mL) under argon at -78 °C was added 0.585 g of NaH (60% dispersed in mineral oil, 0.585 g, 14.6 mmol). After the mixture was stirred for 5 min, MeI (0.55 mL, 8.88 mmol) was added dropwise over 2 min and the reaction mixture allowed to warm to room temperature with stirring over 3 h. Water was added dropwise until effervescence subsided, and the resulting suspension was concentrated to dryness in vacuo. The resulting slurry was diluted with water (50 mL) and acidified to pH 1 using 1 N HCl. The acidified mixture was partitioned against EtOAc (50 mL), the phases were separated, and the aqueous phase was washed with EtOAc (2 × 50 mL). The combined organics were concentrated to dryness in vacuo, and the resulting yellow oil was partitioned between MeOH (50 mL) and pentane (3 × 100 mL) to remove residual mineral oil. The MeOH phase was concentrated to dryness in vacuo to give a yellow solid and purified by C₁₈ RP-HPLC (Agilent Eclipse XDB-C₁₈ 4.6 mm × 150 mm column, 80% MeOH/20% H₂O (acidified with 0.002% formic acid), 1 mL/min, *t*_R = 14.4 min) to give **18** as an amorphous white solid (2.4 mg, 4.7%). To a solution of **18** (0.5 mg, 1 mmol) in dry C₆H₆ (600 μ L) and dry MeOH (150 μ L, 3.71 mmol) was added a solution of

TMS-diazomethane (2 M, 150 μ L, 0.30 mmol) dropwise over 1 min, and the reaction mixture was stirred at room temperature for 12 h. The reactants were evaporated under a stream of N_2 gas, and the product was azeotroped with MeOH (2 \times 5 mL). The solvent was evaporated under a stream of N_2 gas and the resulting solid purified by C_{18} RP-HPLC (Agilent Eclipse XDB- C_{18} 4.6 mm \times 150 mm column, 70–100% MeOH with H_2O /0.002% formic acid over 20 min, 1 mL/min, t_R = 15.5 min) to give **22** as an amorphous white solid (0.28 mg, 56% yield).

Compound 13: white solid; $[\alpha]_D^{20}$ -245 (*c* 0.64, MeOH); UV (MeOH) λ_{max} (log ϵ) 228 (sh) (3.97) nm; IR (NaCl, cm^{-1}) ν_{max} 3255, 2963, 2934, 2873, 1635, 1470, 1400 cm^{-1} ; 1H NMR (CD_3CN , 600 MHz) δ 7.27 (t, *J* = 7.2 Hz, 2H), 7.24 (d, *J* = 7.2 Hz, 1H), 7.19 (t, *J* = 7.2 Hz, 2H), 5.75 (dd, *J* = 9.6, 6 Hz, 1H), 5.39 (q, *J* = 13.5, 6.6 Hz, 1H), 5.13 (d, *J* = 10.8 Hz, 1H), 5.09 (d, *J* = 10.2 Hz, 1H), 4.91 (d, *J* = 10.8 Hz, 1H), 3.07 (dd, *J* = 14.4, 6 Hz, 1H), 2.93 (s, 6H), 2.87 (s, 3H), 2.86 (s, 3H), 2.85 (s, 3H), 2.84 (s, 3H), 2.33 (dt, *J* = 12.6, 7.2, 1.8 Hz, 2H), 2.29–2.24 (m, 3H), 2.22 (s, 3H), 2.19–2.13 (m, 6H), 1.58 (q, *J* = 7.8 Hz, 2H), 1.51 (q, *J* = 8.4 Hz, 2H), 1.42–1.38 (m, 2H), 1.01 (d, *J* = 6 Hz, 3H), 0.84 (dd, *J* = 11.7, 6.4 Hz, 6H), 0.77 (q, *J* = 9, 6.6 Hz, 6H), 0.70 (dd, *J* = 6.8, 2 Hz, 6H); ^{13}C NMR (CD_3CN , 125 MHz) δ 14.7, 18.2, 18.3, 18.5, 18.8, 19.7, 19.9, 20.3, 25.4, 27.8, 27.9, 28.1, 29.2, 29.3, 29.8, 30.7, 30.7, 30.8, 33.9, 35.8, 35.9, 37.3, 50.4, 54.9, 59.0, 59.0, 59.2, 69.7, 85.5, 127.5, 129.3, 130.5, 139.0, 169.6, 170.5, 170.9, 171.1, 171.6, 174.2; HRESIMS m/z [M + Na] $^+$ 775.5094 (calcd for $C_{42}H_{68}N_6O_6Na$, 775.5093).

Compound 14: white solid; $[\alpha]_D^{20}$ -234 (*c* 0.73, MeOH); UV (MeOH) λ_{max} (log ϵ) 224 (sh) (3.94) nm; IR (NaCl, cm^{-1}) ν_{max} 3501, 2963, 2932, 2873, 1727, 1644, 1470, 1400 cm^{-1} ; 1H NMR (CD_3CN , 600 MHz) δ 7.27 (t, *J* = 7.6 Hz, 2H), 7.23 (d, *J* = 8.3 Hz, 2H), 7.19 (t, *J* = 7.1 Hz, 1H), 5.83 (dddd, *J* = 16.8, 10.2, 6.6, 6.6 Hz, 1H), 5.75 (dd, *J* = 9.5, 6.1 Hz, 1H), 5.39 (q, *J* = 13.8, 6.6 Hz, 1H), 5.12 (dd, *J* = 10.8, 2 Hz, 1H), 5.09 (d, *J* = 10.8 Hz, 1H), 5.01 (ddt, *J* = 16.8, 2.4, 1.6 Hz, 1H), 4.92 (ddt, *J* = 10.8, 2.4 Hz, 1.3 Hz, 1H), 4.91 (d, *J* = 10.8 Hz, 1H), 3.07 (dd, *J* = 14.4, 6 Hz, 1H), 2.92 (s, 6H), 2.86 (s, 3H), 2.85 (s, 3H), 2.84 (s, 3H), 2.83 (s, 3H), 2.33–2.14 (m, 2H), 2.27–2.23 (m, 3H), 2.21 (s, 3H), 2.05–2.02 (m, 1H), 1.61 (dt, *J* = 4.7, 2.7, 1.2 Hz, 1H), 1.57–1.52 (m, 3H), 1.40–1.30 (m, 3H), 1.01 (d, *J* = 6.6 Hz, 3H), 0.84 (dd, *J* = 12, 6.6 Hz, 7H), 0.77 (dd, *J* = 9.6, 6.7 Hz, 6H), 0.70 (dd, *J* = 7.2, 3.6 Hz, 6H); ^{13}C NMR (CD_3CN , 125 MHz) δ 14.7, 18.2, 18.2, 18.3, 18.5, 19.7, 19.8, 19.9, 20.3, 25.7, 27.8, 27.9, 28.0, 29.5, 29.6, 29.7, 29.9, 30.7, 30.8, 33.0, 33.9, 34.0, 34.4, 35.8, 35.9, 37.2, 50.4, 54.8, 58.9, 59.0, 59.2, 114.9, 125.8, 127.4, 129.3, 130.4, 132.2, 139.0, 140.1, 169.5, 170.5, 170.8, 171.1, 171.6, 174.2; HRESIMS m/z [M + Na] $^+$ 777.5256 (calcd for $C_{42}H_{70}N_6O_6Na$, 777.5249).

Compound 15: white solid; $[\alpha]_D^{20}$ -274 (*c* 0.86, MeOH); UV (MeOH) λ_{max} (log ϵ) 228 (sh) (4.00) nm; IR (NaCl, cm^{-1}) ν_{max} 3501, 3255, 2964, 2934, 2874, 1633, 1470, 1402 cm^{-1} ; 1H NMR (CD_3CN , 600 MHz) δ 7.27 (t, *J* = 7.2 Hz, 2H), 2.24 (d, *J* = 7.2 Hz, 2H), 7.19 (t, *J* = 7.2 Hz, 1H), 5.75 (dd, *J* = 9.6, 6 Hz, 1H), 5.38 (q, *J* = 13.8, 6.6 Hz, 1H), 5.12 (d, *J* = 10.8 Hz, 1H), 5.09 (d, *J* = 10.8 Hz, 1H), 4.91 (d, *J* = 10.8 Hz, 1H), 3.06 (dd, *J* = 14.4, 6 Hz, 1H), 2.93 (s, 3H), 2.87 (s, 3H), 2.86 (s, 3H), 2.84 (s, 3H), 2.83 (s, 3H), 2.35 (dt, *J* = 13.2, 7.2, 1.8 Hz, 2H), 2.27–2.23 (m, 3H), 2.21 (s, 3H), 2.19 (dt, *J* = 11.4 Hz, 7.7, 2.4 Hz, 2H), 2.15 (t, *J* = 2.6 Hz, 1H), 1.64 (q, *J* = 7.2 Hz, 2H), 1.51 (q, *J* = 7.8 Hz, 2H), 1.01 (d, *J* = 6.6 Hz, 3H), 0.84 (dd, *J* = 10.8, 6.6 Hz, 7H), 0.77 (dd, *J* = 7.8, 6.6 Hz, 7H), 0.70 (dd, *J* = 7.2, 2.1 Hz, 7H); ^{13}C NMR (CD_3CN , 125 MHz) δ 14.6, 18.2, 18.3, 18.5, 18.6, 19.7, 19.9, 20.3, 25.0, 27.8, 27.9, 28.1, 28.9, 29.7, 30.7, 30.8, 30.9, 33.5, 35.8, 35.9, 37.2, 50.4, 54.8, 59.0, 59.1, 59.2, 69.8, 85.2, 127.4, 129.3, 130.4, 139.0, 169.5, 170.5, 170.8, 171.1, 171.6, 174.0; HRESIMS m/z [M + Na] $^+$ 761.4935 (calcd for $C_{41}H_{66}N_6O_6Na$, 761.4936).

Compound 16: white solid; $[\alpha]_D^{20}$ -227 (*c* 0.22, MeOH); UV (MeOH) λ_{max} (log ϵ) 225 (sh) (4.00) nm; IR (NaCl, cm^{-1}) ν_{max}

3501, 2963, 2931, 2873, 1639, 1470, 1400 cm^{-1} ; 1H NMR (CD_3CN , 600 MHz) δ 7.27 (t, *J* = 7.2 Hz, 2H), 7.23, (d, *J* = 7.2 Hz, 2H), 7.19 (t, *J* = 7.2 Hz, 1H), 5.82 (dddd, *J* = 13.8, 10.8, 6.6, 6.6 Hz, 1H), 5.74 (dd, *J* = 9.6, 6 Hz, 1H), 5.38 (q, *J* = 13.4, 6.6 Hz, 1H), 5.12 (d, *J* = 10.8 Hz, 1H), 5.09 (d, *J* = 10.8 Hz, 1H), 5.01 (ddt, *J* = 17.1, 2.2 Hz, 1.6 Hz, 1H), 4.93 (ddt, *J* = 10.2, 2.2, 1.2 Hz, 1H), 4.91 (d, *J* = 10.8 Hz, 1H), 3.06 (dd, *J* = 14.2, 6 Hz, 1H), 2.92 (s, 6H), 2.86 (s, 3H), 2.85 (s, 3H), 2.84 (s, 3H), 2.83 (s, 3H), 2.33 (dt, *J* = 10.8, 7.8, 4.2 Hz, 2H), 2.26–2.23 (m, 3H), 2.21 (s, 3H), 2.07–2.04 (m, 2H), 1.56 (q, *J* = 7.2 Hz, 2H), 1.39 (q, *J* = 7.2 Hz, 2H), 1.01 (d, *J* = 7.2 Hz, 3H), 0.84 (dd, *J* = 12, 6.6 Hz, 7H), 0.76 (dd, *J* = 9.5, 6.6 Hz, 6H), 0.70 (dd, *J* = 6.6, 3.6 Hz, 6H); ^{13}C NMR (CD_3CN , 125 MHz) δ 14.6, 18.2, 18.3, 18.5, 19.7, 19.9, 20.3, 25.3, 27.8, 27.9, 28.0, 29.3, 29.7, 30.7, 30.8, 30.9, 33.9, 34.2, 35.8, 35.9, 37.2, 50.4, 54.8, 58.9, 59.0, 59.2, 115.0, 127.4, 129.3, 130.4, 139.0, 139.9, 169.5, 170.5, 170.5, 171.1, 171.6, 174.2; HRESIMS m/z [M + Na] $^+$ 763.5092 (calcd for $C_{41}H_{68}N_6O_6Na$, 763.5093).

Compound 17: white solid; $[\alpha]_D^{20}$ -200 (*c* 0.2, MeOH); UV (MeOH) λ_{max} (log ϵ) 228 (sh) (3.85) nm; IR (NaCl, cm^{-1}) ν_{max} 3307, 2963, 1738, 1639, 1470, 1403 cm^{-1} ; 1H NMR (CD_3OD , 600 MHz) δ 7.32–7.28 (m, 2H), 7.24–7.21 (m, 3H), 5.35 (q, *J* = 13.2, 6.6 Hz, 1H), 5.12 (d, *J* = 10.8 Hz, 1H), 5.08 (d, *J* = 10.8 Hz, 1H), 4.85 (d, *J* = 10.8 Hz, 1H), 3.01 (s, 3H), 2.96 (s, 3H), 2.93 (s, 3H), 2.81 (s, 3H), 2.44–2.42 (m, 3H), 2.35–2.26 (m, 3H), 2.19–2.18 (m, 3H), 2.14 (s, 3H), 1.62 (q, *J* = 7.8 Hz, 2H), 1.52 (q, *J* = 7.8 Hz, 2H), 1.46 (q, *J* = 7.8 Hz, 2H), 1.07 (d, *J* = 7.8 Hz, 2H), 0.90–0.86 (m, 6H), 0.84–0.81 (m, 7H), 0.77–0.73 (m, 6H); ^{13}C NMR (CD_3OD , 125 MHz) δ 14.3, 18.4, 18.6, 19.0, 19.7, 20.0, 20.4, 20.6, 25.8, 28.3, 28.5, 28.6, 28.7, 29.6, 30.0, 31.0, 31.1, 31.2, 31.3, 34.4, 36.3, 50.2, 51.3, 59.8, 60.0, 69.7, 84.9, 120.1, 128.1, 129.8, 130.2, 130.5, 138.7, 129.3, 170.2, 171.7, 171.8, 172.5, 172.6, 176.2; HRESIMS m/z [M + Na] $^+$ 748.4614 (calcd for $C_{40}H_{63}N_5O_7Na$, 748.4620).

Compound 18: white solid; $[\alpha]_D^{20}$ -243 (*c* 0.7, MeOH); UV (MeOH) λ_{max} (log ϵ) 225 (sh) (3.95) nm; IR (NaCl, cm^{-1}) ν_{max} 3445, 2964, 2932, 2874, 1737, 1640, 1470, 1403 cm^{-1} ; 1H NMR (CD_3CN , 600 MHz) δ 7.32–7.29 (m, 2H), 7.24–7.19 (m, 3H), 5.82 (dddd, *J* = 16.2 Hz, 10.2 Hz, 6.6 Hz, 6.6 Hz, 1H), 5.37–5.33 (m, 1H), 5.12 (d, *J* = 10.8 Hz, 1H), 5.08 (d, *J* = 10.8 Hz, 1H), 5.01–4.97 (m, 1H), 4.93–4.91 (m, 1H), 4.85 (d, *J* = 10.2 Hz, 1H), 2.91 (s, 3H), 2.85 (s, 6H), 2.72 (s, 3H), 2.33–2.30 (m, 2H), 2.28–2.21 (m, 4H), 2.05–2.02 (m, 3H), 1.55 (q, *J* = 7.2 Hz, 2H), 1.38 (q, *J* = 7.2 Hz, 2H), 1.32 (q, *J* = 7.2 Hz, 2H), 1.01 (d, *J* = 6 Hz, 2H), 0.84–0.81 (m, 6H), 0.76 (bd, *J* = 6.6 Hz, 7H), 0.69 (bd, *J* = 6.6 Hz, 6H); ^{13}C NMR (CD_3CN , 125 MHz) δ 14.4, 18.1, 18.3, 18.5, 19.7, 19.8, 19.9, 20.2, 25.7, 27.7, 27.8, 27.9, 28.0, 29.6, 30.3, 30.7, 30.8, 30.9, 33.0, 34.0, 34.4, 34.9, 35.6, 49.9, 50.5, 59.0, 59.1, 59.6, 114.9, 127.7, 129.5, 130.0, 130.2, 138.8, 140.1, 169.4, 170.8, 171.6, 172.1, 172.1, 174.3; HRESIMS m/z [M + Na] $^+$ 750.4771 (calcd for $C_{40}H_{65}N_5O_7Na$, 750.4776).

Compound 19: white solid; $[\alpha]_D^{20}$ -160 (*c* 0.18, MeOH); UV (MeOH) λ_{max} (log ϵ) 226 (sh) (3.90) nm; IR (NaCl, cm^{-1}) ν_{max} 3472, 3257, 2964, 2874, 1733, 1639, 1470, 1403 cm^{-1} ; 1H NMR (CD_3CN , 600 MHz) δ 7.32–7.29 (m, 2H), 7.28–7.22 (m, 3H), 5.36 (q, *J* = 12, 6.6 Hz, 1H), 5.26 (bs, 1H), 5.12 (d, *J* = 10.8 Hz, 1H), 5.08 (d, *J* = 10.8 Hz, 1H), 4.85 (d, *J* = 10.2 Hz, 1H), 2.92 (s, 3H), 2.85 (s, 6H), 2.72 (s, 3H), 2.35 (dt, *J* = 13.2, 7.2, 1.8 Hz, 2H), 2.28–2.22 (m, 4H), 2.20–2.17 (m, 2H), 2.15 (t, *J* = 2.4 Hz, 1H), 2.13 (s, 3H), 1.64 (q, *J* = 7.2 Hz, 2H), 1.51 (q, *J* = 7.2 Hz, 2H), 1.01 (d, *J* = 6.6 Hz, 2H), 0.84–0.78 (m, 6H), 0.77 (bd, *J* = 6.6 Hz, 7H), 0.70–0.66 (m, 8H); ^{13}C NMR (CD_3CN , 125 MHz) δ 14.4, 18.2, 18.3, 18.6, 19.7, 19.8, 19.9, 20.2, 25.1, 27.7, 27.9, 28.1, 29.6, 30.4, 30.7, 32.9, 33.5, 35.0, 49.6, 50.6, 59.0, 59.1, 59.5, 69.8, 85.2, 127.6, 127.8, 129.5, 130.0, 130.2, 138.5, 138.9, 169.4, 169.9, 170.8, 171.5, 172.1, 174.0; HRESIMS m/z [M + Na] $^+$ 734.4456 (calcd for $C_{39}H_{61}N_5O_7Na$, 734.4463).

Compound 20: white solid; $[\alpha]_D^{20}$ -200 (*c* 0.20, MeOH); UV (MeOH) λ_{max} (log ϵ) 223 (sh) (3.93) nm; IR (NaCl, cm^{-1}) ν_{max} 3401, 2963, 2932, 2873, 1733, 1639, 1470, 1403 cm^{-1} ; 1H NMR

(CD₃OD, 600 MHz) δ 7.33–7.28 (m, 2H), 7.26–7.21 (m, 3H), 5.81 (dddd, $J = 17.4, 10.2, 6.6, 6.6$ Hz, 1H), 5.43 (q, $J = 12.6, 6.6$ Hz, 1H), 5.17 (d, $J = 10.8$ Hz, 1H), 5.13 (d, $J = 10.8$ Hz, 1H), 5.02–4.98 (m, 1H), 4.95–4.92 (m, 1H), 4.88 (s, 1H), 4.84 (s, 1H), 3.01 (s, 3H), 2.96 (s, 6H), 2.80 (s, 3H), 2.44–2.41 (m, 2H), 2.34–2.26 (m, 3H), 2.11 (s, 3H), 2.09–2.06 (m, 4H), 1.62 (q, $J = 7.2$ Hz, 2H), 1.45 (q, $J = 7.2$ Hz, 2H), 1.06 (d, $J = 6$ Hz, 2H), 0.92–0.87 (m, 6H), 0.84–0.80 (m, 8H), 0.76–0.73 (m, 6H); ¹³C NMR (CD₃OD, 125 MHz) δ 14.3, 18.4, 18.6, 18.6, 19.7, 19.8, 20.0, 20.4, 20.6, 25.8, 28.3, 28.4, 28.6, 28.7, 29.8, 29.9, 30.5, 31.1, 31.2, 34.4, 34.7, 50.2, 51.4, 59.8, 59.9, 115.2, 128.1, 129.8, 130.2, 130.5, 138.7, 129.4, 139.7, 170.2, 120.3, 171.8, 172.5, 173.0, 176.3; HRESIMS m/z [M + Na]⁺ 736.4610 (calcd for C₃₉H₆₃N₅O₇Na, 736.4620).

Compound 21: white solid; $[\alpha]_D^{20} -132$ (c 0.43, MeOH); UV (MeOH) λ_{\max} (log ϵ) 225 (sh) (3.90) nm; IR (NaCl, cm⁻¹) ν_{\max} 3309, 2961, 2931, 2873, 1738, 1639, 1462, 1403 cm⁻¹; ¹H NMR (CD₃CN, 600 MHz) δ 7.12–7.28 (m, 2H), 7.25–7.20 (m, 3H), 5.37 (q, $J = 13.2, 6.6$ Hz, 1H), 5.22 (dd, $J = 12, 7.2$ Hz, 1H), 5.12 (d, $J = 10.2$ Hz, 1H), 5.09 (d, $J = 10.8$ Hz, 1H), 4.87 (d, $J = 10.2$ Hz, 1H), 3.68 (s, 3H), 2.92 (s, 3H), 2.85 (s, 6H), 2.70 (s, 3H), 2.33 (tt, $J = 7.2, 1.8$ Hz, 3H), 2.28–2.22 (m, 4H), 2.17 (s, 3H), 1.57 (q, $J = 7.8$ Hz, 2H), 1.50 (q, $J = 7.2$ Hz, 2H), 1.39 (q, $J = 7.2$ Hz, 2H), 1.01 (d, $J = 7.2$ Hz, 2H), 0.83–0.75 (m, 13H), 0.70–0.68 (m, 6H); ¹³C NMR (CD₃CN, 125 MHz) δ 14.4, 18.2, 18.4, 18.5, 18.8, 19.7, 19.9, 20.3, 23.8, 24.6, 25.4, 27.8, 28.0, 28.1, 29.2, 29.3, 29.8, 30.7, 30.8, 31.2, 33.1, 34.0, 35.0, 39.7, 50.5, 52.8, 59.0, 59.2, 69.7, 85.5, 127.7, 129.6, 130.0, 138.7, 169.5, 170.9, 171.6, 171.9, 172.0, 174.2; HRESIMS m/z [M + Na]⁺ 762.4765 (calcd for C₄₁H₆₅N₅O₇Na, 762.4776).

Compound 22: white solid; $[\alpha]_D^{20} -157$ (c 0.69, MeOH); UV (MeOH) λ_{\max} (log ϵ) 227 (sh) (4.00) nm; IR (NaCl, cm⁻¹) ν_{\max} 3473, 2962, 2931, 2873, 1741, 1640, 1463, 1403 cm⁻¹; ¹H NMR (CD₃CN, 600 MHz) δ 7.31–7.28 (m, 2H), 7.25–7.20 (m, 3H), 5.83 (dddd, $J = 17.4, 10.2, 6.6, 6.6$ Hz, 1H), 5.38 (q, $J = 13.2, 6.6$ Hz, 1H), 5.24 (dd, $J = 12, 4.8$ Hz, 1H), 5.12 (d, $J = 10.8$ Hz, 1H), 5.09 (d, $J = 10.8$ Hz, 1H), 5.02–4.96 (m, 1H), 4.94–4.92 (m, 1H), 4.87 (d, $J = 10.8$ Hz, 1H), 3.68 (s, 3H), 2.92 (s, 3H), 2.85 (s, 6H), 2.70 (s, 3H), 2.33–2.30 (m, 2H), 2.28–2.21 (m, 4H), 2.17 (s, 3H), 2.05–2.03 (m, 2H), 1.55 (q, $J = 7.2$ Hz, 2H), 1.38 (q, $J = 7.2$ Hz, 2H), 1.31 (q, $J = 7.2$ Hz, 2H), 1.01 (d, $J = 6.6$ Hz, 2H), 0.82 (dd, $J = 9, 6.6$ Hz, 6H), 0.79–0.75 (m, 7H), 0.69 (dd, $J = 6.6, 2.4$ Hz, 6H); ¹³C NMR (CD₃CN, 125 MHz) δ 14.4, 18.1, 18.3, 18.5, 19.7, 19.9, 20.2, 23.7, 24.6, 25.7, 27.7, 27.9, 28.1, 29.5, 29.6, 30.5, 30.7, 31.2, 33.0, 34.0, 34.4, 34.9, 39.7, 50.4, 52.8, 58.9, 59.1, 59.6, 68.7, 114.9, 127.7, 129.5, 130.0, 132.3, 140.1, 169.4, 170.8, 171.6, 171.9, 171.9, 174.2; HRESIMS m/z [M + Na]⁺ 764.4930 (calcd for C₄₁H₆₇N₅O₇Na, 764.4933).

Compound 23: white solid; $[\alpha]_D^{20} -145$ (c 0.34, MeOH); UV (MeOH) λ_{\max} (log ϵ) 225 (sh) (3.93) nm; IR (NaCl, cm⁻¹) ν_{\max} 3308, 2962, 2873, 1739, 1639, 1462, 1403 cm⁻¹; ¹H NMR (CD₃CN, 600 MHz) δ 7.34–7.28 (m, 2H), 7.25–7.20 (m, 3H), 5.36 (q, $J = 13.2, 6.6$ Hz, 1H), 5.23 (dd, $J = 12, 4.7$ Hz, 1H), 5.12 (d, $J = 10.8$ Hz, 1H), 5.09 (d, $J = 10.6$ Hz, 1H), 4.87 (d, $J = 10.2$ Hz, 1H), 3.68 (s, 3H), 2.92 (s, 3H), 2.85 (s, 6H), 2.70 (s, 3H), 2.35 (dt, $J = 13.2, 7.2$ Hz, 1.8 Hz, 2H), 2.27–2.23 (m, 4H), 2.22–2.18 (m, 3H), 2.17 (s, 3H), 1.64 (q, $J = 7.8$ Hz, 2H), 1.51 (q, $J = 7.8$ Hz, 2H), 1.01 (d, $J = 7.2$ Hz, 2H), 0.83–0.80 (m, 6H), 0.79–0.76 (m, 7H), 0.70–0.68 (m, 6H); ¹³C NMR (CD₃CN, 125 MHz) δ 14.4, 18.3, 18.5, 18.6, 19.7, 19.9, 20.2, 23.7, 24.6, 25.0, 27.7, 27.9, 28.1, 28.9, 29.7, 30.7, 30.8, 31.2, 33.5, 34.9, 39.7, 50.4, 52.8, 59.0, 59.6, 69.8, 85.2, 116.1, 127.7, 129.5, 130.0, 130.3, 132.3, 138.7, 169.4, 170.8, 171.6, 171.9, 171.9, 174.0; HRESIMS m/z [M + Na]⁺ 748.4614 (calcd for C₄₀H₆₃N₅O₇Na, 748.4620).

Compound 24: white solid; $[\alpha]_D^{20} -149$ (c 0.36, MeOH); UV (MeOH) λ_{\max} (log ϵ) 227 (sh) (3.82) nm; IR (NaCl, cm⁻¹) ν_{\max} 3307, 2962, 2931, 2873, 1739, 1640, 1463, 1403 cm⁻¹; ¹H NMR (CD₃CN, 600 MHz) δ 7.31–7.28 (m, 2H), 7.25–7.20 (m, 3H), 5.83 (dddd, $J = 16.8, 10.2, 6.6, 6.6$ Hz, 1H), 5.37 (q, $J = 13.2, 6.6$ Hz, 1H), 5.24 (dd, $J = 12, 4.8$ Hz, 1H), 5.12 (d, $J = 10.8$ Hz, 1H),

5.09 (d, $J = 10.8$ Hz, 1H), 5.02–4.98 (m, 1H), 4.94–4.92 (m, 1H), 4.87 (d, $J = 10.2$ Hz, 1H), 3.68 (s, 3H), 2.92 (s, 3H), 2.85 (s, 6H), 2.70 (s, 3H), 2.34–2.31 (m, 3H), 2.17 (s, 3H), 2.07–2.04 (m, 3H), 1.56 (q, $J = 7.2$ Hz, 3H), 1.39 (q, $J = 7.2$ Hz, 3H), 1.01 (d, $J = 6.6$ Hz, 2H), 0.84–0.79 (m, 6H), 0.78–0.75 (m, 7H), 0.69 (dd, $J = 6.6, 2.4$ Hz, 6H); ¹³C NMR (CD₃CN, 125 MHz) δ 14.4, 18.1, 18.3, 18.5, 19.7, 19.9, 20.2, 23.7, 24.6, 25.3, 27.7, 27.9, 28.1, 29.3, 30.7, 30.8, 31.2, 33.8, 34.9, 39.7, 50.4, 52.8, 59.0, 59.1, 59.6, 61.6, 63.3, 68.7, 115.0, 127.7, 129.5, 129.7, 130.0, 132.3, 139.9, 170.8, 170.9, 171.6, 171.9, 171.9, 174.2; HRESIMS m/z [M + Na]⁺ 750.4773 (calcd for C₄₀H₆₅N₅O₇Na, 750.4776).

Acknowledgment. We thank the Government of Panama for support of the ICBG program, H.-E. Högborg for the provision of authentic standards of (2*R*)- and (2*S*)-methyl-octanoic acid, A. Lawrence and the staff of the Smithsonian Tropical Research Institute Bocas del Toro Field Station for assistance with field collections, and R. Okuda for assistance with optical rotation measurements. X-ray analysis was performed by A. Rheingold at the UCSD Department of Chemistry Small Molecule X-ray Facility. Financial support was provided by the Fogarty International Center's International Cooperative Biodiversity Group (ICBG) program in Panama (Grant ICBG TW006634), UCSC startup funds, and the Panamanian Ministry of Science (SENACYT, Grant EST06-O-022). L.M.S. is supported by an NSF Graduate Research Fellowship.

Supporting Information Available: ¹H and ¹³C NMR spectra of **1–4** and **9–24**, structure determination of subunits **a–f**, HRESIMS fragmentation interpretation for **11** and **12**, and ORTEP diagram for **9**; CIF data for **9**. This material is available free of charge via the Internet at <http://pubs.acs.org>.

References

- (1) Cavalli, A.; Bolognesi, M. L. Neglected Tropical Diseases: Multi-Target-Directed Ligands in the Search for Novel Lead Candidates against Trypanosoma and Leishmania. *J. Med. Chem.* **2009**, *52*, 7339–7359.
- (2) Croft, S. L.; Sundar, S.; Fairlamb, A. H. Drug Resistance in Leishmaniasis. *Clin. Microbiol. Rev.* **2006**, *19*, 111–126.
- (3) Chappuis, F.; Sundar, S.; Hailu, A.; Ghalib, H.; Rijal, S.; Peeling, R. W.; Alvar, J.; Boelaert, M. Visceral Leishmaniasis: What Are the Needs for Diagnosis, Treatment and Control? *Nat. Rev. Microbiol.* **2007**, *5*, 873–882.
- (4) Bern, C.; Maguire, J. H.; Alvar, J. Complexities of Assessing the Disease Burden Attributable to Leishmaniasis. *PLoS Neglected Trop. Dis.* **2008**, *2*, e313.
- (5) Reithinger, R. Leishmaniasis' Burden of Disease: Ways Forward for Getting from Speculation to Reality. *PLoS Neglected Trop. Dis.* **2008**, *2*, e285.
- (6) Martínez-Luis, S.; Della-Togna, G.; Coley, P. D.; Kursar, T. A.; Gerwick, W. H.; Cubilla-Rios, L. Antileishmanial Constituents of the Panamanian Endophytic Fungus *Edenia* sp. *J. Nat. Prod.* **2008**, *71*, 2011–2014.
- (7) Montenegro, H.; Gutierrez, M.; Romero, L. I.; Ortega-Barria, E.; Capson, T. L.; Cubilla Rios, L. Aporphine Alkaloids from *Guatteria* spp. with Leishmanicidal Activity. *Planta Med.* **2003**, *69*, 677–679.
- (8) Harada, K.; Fujii, K.; Mayumi, T.; Hibino, Y.; Suzuki, M.; Ikai, Y.; Oka, H.; Method, A. Using LC/MS for Determination of Absolute Configuration of Constituent Amino Acids in Peptide—Advanced Marfey's Method. *Tetrahedron Lett.* **1995**, *36*, 1515–1518.
- (9) Reese, M. T.; Gulavita, N. K.; Nakao, Y.; Hamann, M. T.; Yoshida, W. Y.; Coval, S. J.; Scheuer, P. J. Kulolide: A Cytotoxic Dipeptide from a Cephalaspidean Mollusk, *Philinopsis speciosa*. *J. Am. Chem. Soc.* **1996**, *118*, 11081–11084.
- (10) Chen, H.; Feng, Y.; Xu, Z.; Ye, T. The Total Synthesis and Reassignment of Stereochemistry of Dragonamide. *Tetrahedron* **2005**, *61*, 11132–11140.
- (11) McPhail, K. L.; Correa, J.; Linington, R. G.; Gonzalez, J.; Ortega-Barria, E.; Capson, T. L.; Gerwick, W. H. Antimalarial Linear

- Lipopeptides from a Panamanian Strain of the Marine Cyanobacterium *Lynghya majuscula*. *J. Nat. Prod.* **2007**, *70*, 984–988.
- (12) Kwan, D. H.; Sun, Y.; Schulz, F.; Hong, H.; Popovic, B.; Sim-Stark, J. C. C.; Haydock, S. F.; Leadlay, P. F. Prediction and Manipulation of the Stereochemistry of Enoylreduction in Modular Polyketide Synthases. *Chem. Biol.* **2008**, *15*, 1231–1240.
- (13) Edwards, D. J.; Marquez, B. L.; Nogle, L. M.; McPhail, K.; Goeger, D. E.; Roberts, M. A.; Gerwick, W. H. Structure and Biosynthesis of the Jamaicamides, New Mixed Polyketide–Peptide Neurotoxins from the Marine Cyanobacterium *Lynghya majuscula*. *Chem. Biol.* **2004**, *11*, 817–833.
- (14) Biron, E.; Chatterjee, J.; Ovadia, O.; Langenegger, D.; Brueggen, J.; Hoyer, D.; Schmid, H. A.; Jelnick, R.; Gilon, C.; Hoffman, A.; Kessler, H. Improving Oral Bioavailability of Peptides by Multiple N-Methylation: Somatostatin Analogues. *Angew. Chem., Int. Ed.* **2008**, *47*, 2595–2599.
- (15) Chatterjee, J.; Gilon, C.; Hoffman, A.; Kessler, H. N-Methylation of Peptides: A New Perspective in Medicinal Chemistry. *Acc. Chem. Res.* **2008**, *41*, 1331–1342.
- (16) Major and minor conformers observed in both CD₃CN and CD₂Cl₂ when acquired at 25 °C.
- (17) Geitler, L. *Cyanophyceae.*; Koeltz Scientific Books: Koenigstein, Germany, 1932.
- (18) Corbett, Y.; Herrera, L.; Gonzalez, J.; Cubilla, L.; Capson, T. L.; Coley, P. D.; Kursar, T. A.; Romero, L. I.; Ortega-Barria, E. A novel DNA-based microfluorimetric method to evaluate antimalarial drug activity. *Am. J. Trop. Med. Hyg.* **2004**, *70*, 119–124.
- (19) Buckner, F. S.; Verlinde, C. L.; La Flamme, A. C.; Van Voorhis, W. C. Efficient technique for screening drugs for activity against *Trypanosoma cruzi* using parasites expressing beta-galactosidase. *Antimicrob. Agents Chemother.* **1996**, *40*, 2592–2597.
- (20) Calderon, A.; Romero, L. I.; Ortega-Barria, E.; Brun, R.; Correa, M. A.; Gupta, M. P. Evaluation of larvicidal and in vitro antiparasitic activities of plants in a biodiversity plot in the Altos de Campana National Park, Panama. *Pharm. Biol.* **2006**, *44*, 487–498.